DOI: 10.5281/zenodo.17112206

CHAPTER 8

Different Characterization Techniques and Physical Parameters Useful for Materials Analysis

Ravindra N. Chikhale

Department of Physics, J.S.M. College, Alibag, Raigad 402201 Maharashtra, India

Corresponding author Email: chikhaleravi@gmail.com

Received: 05 September 2025; Accepted: 12 September 2025; Available online: 13 September 2025

Abstract: The XRD technique provides information about various structural parameters, including crystallite size, internal strain (stress), crystal structure, interatomic spacing (i.e., interplanar distance), and lattice plane orientation. It confirms the presence of impurity phases in the crystal. The different characteristic peaks of the FTIR spectrum of the sample identify the presence of different groups, molecules, and give information about the crystal structure. SEM and FE-SEM are useful techniques to confirm the morphology of the sample and material composition. The two-probe method is very useful to measure the DC electrical resistivity of the sample. Dielectric parameters confirm dielectric behaviour of the sample. The VSM is used for the investigation of magnetic properties of materials, and we can estimate different magnetic parameters such as saturation magnetization, coercivity, retentivity, and isotropic constant.

Materials Science: Advances in Synthesis, Characterization and Applications (Vol. 1) - Digambar M. Sapkal, Harshal M. Bachhav, Gaurav Mahadev Lohar, Sanjay P. Khairnar (Eds.)

ISBN: 978-93-95369-55-8 (paperback) 978-93-95369-46-6 (electronic) | © 2025 Advent Publishing.

https://doi.org/10.5281/zenodo.17112206

Keywords: XRD, FTIR, EDS, DC resistivity, dielectric properties, VSM

A. Introduction

Researchers restlessly try to develop different materials with improved properties and performance of the material. The properties and performance of materials depend on the method of preparation, environmental condition, and sintering temperature. Methods for material characterization are very important. Applications of the material in science and technology depends on structural, morphological, electrical, dielectric and magnetic parameters.

In this chapter we have discussed X-ray diffraction (XRD) technique useful for structural analysis and how to finding different structural parameters like crystallite size, lattice parameters, bond lengths, hopping lengths, ionic radii, lattice strain, X-ray density etc. Fourier transform spectroscopy (FTIR) provide information about different bonds formed in the material and confirm formation of the crystal structure. Field emission scanning electron microscopy (FE-SEM) is basic characterization technique used for morphological study and confirm grain formation and helpful to find grain size.

To perform optical analysis Ultra-violet visible (UV-Vis) technique is useful. The compositional analysis can perform from energy dispersive spectroscopy (EDS). Two probe method is used to measure DC electrical resistivity and from Arrhenius relation we can calculate activation energy. The dielectric parameters are depending on the frequency of the applied electric field. Dielectric parameters confirm dielectric behaviour of the sample. To study magnetic properties of the material vibrating sample magnetometer is very useful. From magnetization against magnetic field curve we can estimate different magnetic parameters like saturation magnetization, remanent magnetization, coercivity and anisotropic constant etc.

B. Characterization techniques

1. X-ray diffraction (XRD) technique

XRD is a very important technique in science and technology. This technique is based on the principle of constructive interference when a monochromatic X - ray beam incident on a sample. Figure 1 shows a ray diagram of the XRD technique [1].

X-ray diffraction equipment consists of an X-ray source, sample on specimen, and detector. When X-ray emitted by X-ray source incident on sample get diffracted in possible direction. This diffracted ray satisfied Bragg's diffraction condition [2]

$$2d \sin\theta = n\lambda \qquad (1)$$

Where, d = inter-planar spacing, θ = angle of diffraction,

and λ = wavelength of incident X - rays.

ISBN: 978-93-95369-55-8 (paperback) 978-93-95369-46-6 (electronic)

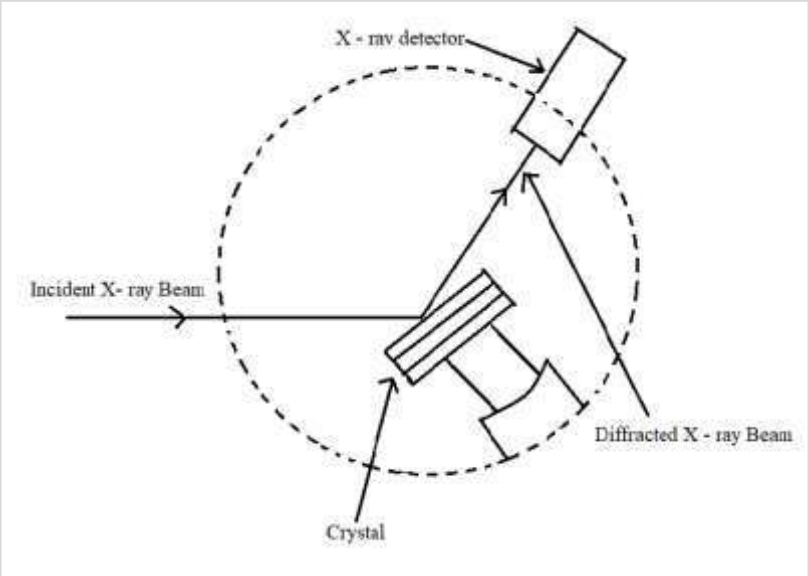

Fig. 1. X-ray diffraction technique

The diffracted rays are detected and recorded by using an X-ray detector as a function of 2θ which is movable on a circular path shown in figure 1. If the XRD spectrum was recorded as the intensity of X-ray against 2θ it gives structural information of the sample. The XRD technique provides useful information about crystallite size, internal strain (stress), crystal structure, interatomic spacing i.e. interplanar distance, lattice plane orientation, and impurity phase present in the crystal. By XRD technique we can following parameters.

The crystallite size (D) and lattice strain (ε)

- **Scherrer Method**

Using this method the we can calculate crystallite size (D) of the particle [3].

$$D = \frac{K\lambda}{\beta_{hkl}\cos\theta} \tag{2}$$

Where, K = Scherrer constant which has a value of 0.94 for a cubic system.

λ = wavelength of incident X-ray = 1.54 Å.

β_{hkl} = full-width at half-maxima (FWHM).

θ = Bragg's angle.

ISBN: 978-93-95369-55-8 (paperback) 978-93-95369-46-6 (electronic) | © 2025 Advent Publishing.

- **Modified Scherrer Method**

Rearranging equation (2), hence

$$\beta_{hkl} = \left(\frac{K\lambda}{D}\right)\left(\frac{1}{\cos\theta}\right) \tag{3}$$

Now take ln of both sides of the equation (3) then the equation becomes

$$\ln \beta_{hkl} = \ln\left(k\lambda / D\right) + \ln\left(1/\cos\theta\right) \tag{4}$$

Plot a graph of $\ln \beta_{hkl}$ Vs $\ln\left(1/\cos\theta\right)$, and fit linearly. The intercept on the $\ln \beta_{hkl}$ axis gives $\ln\left(k\lambda / D\right)$. Hence, from intercept we can calculate average crystalline size [4].

- **Williamson - Hall (W-H) Method**

The lattice strain induced in nanomaterials is due to crystal defects and distortion of the crystal. The lattice strain is represented by following relation [5].

$$\varepsilon = \frac{\beta_{\varepsilon}}{4\tan\theta} \tag{5}$$

Peak broadening in X - ray pattern depends on crystallite size (grain size) and strain present in nanoparticles. Williamson-Hall first time noted equation for FWHM (β_{hkl}) which is resultant of crystallite size (β_D) and lattice strain (β_{ε}) called as Williamson – Hall relation expressed by Lorentzian profile and mathematically, written as [6]

$$\beta_{hkl} = \beta_D + \beta_{\varepsilon} \tag{6}$$

From equations (3) and (5) the equation (6) becomes

$$\beta_{hkl} = \frac{K\lambda}{D\cos\theta} + \frac{4\varepsilon\sin\theta}{\cos\theta} \tag{7}$$

$$\beta_{hkl}\cos\theta = \frac{K\lambda}{D} + 4\varepsilon\sin\theta \tag{8}$$

Plot a graph of $\beta_{hkl}\cos\theta$ Vs $4\sin\theta$ and fit linearly. From the vertical axis (Y) intercept calculate crystallite size.

$$\frac{K\lambda}{D} = \text{ intercept on Y-axis}$$

$D =$ $K\lambda$ /intercept on Y-axis

ISBN: 978-93-95369-55-8 (paperback) 978-93-95369-46-6 (electronic)

$K =$ is constant (0.94 for the spherical shape of the particles)

$\lambda =$ wavelength of the incident X -ray = 1.54 Å

- **Size – Strain (S-S) Method**

In the **W-H** method, lattice strain is considered a uniform in all directions and contribution due to strain is the Lorentzian function. Size-strain method corrected this approximation by considering the non-uniform nature and represented it by the Gaussian function. The Size – Strain relation mathematically written as [7]

$$(d_{hkl}\beta_{hkl}\cos\theta)^2 = (\frac{k\lambda}{D})(d_{hkl}^2\beta_{hkl}\cos\theta) + (\frac{\varepsilon}{2})^2 \quad (9)$$

Where, $d_{hkl} =$ interplanar spacing, $k = 0.94$

Plot a graph of $\left(d_{hkl}\beta_{hkl}\cos\theta\right)^2$ against $\left(d_{hkl}^2\beta_{hkl}\cos\theta\right)$ and fit linearly. We can calculate crystallite size (D) and lattice strain (ε) from slope and intercept on the vertical axis respectively.

$$\text{Slope} = \frac{k\lambda}{D} \quad (10)$$

$$\text{Intercept on the vertical axis} = \frac{\varepsilon^2}{4} \quad (11)$$

Interplanar Distance (d)

To calculate interplanar spacing (d) Use Bragg's law [2].

For first-order diffraction n =1

Therefore,

$$d = \frac{\lambda}{2\sin\theta} \quad (12)$$

Where, $d =$ interplanar spacing, $\theta =$ is angle of diffraction,

$\lambda =$ wavelength of incident X - ray $=$ 1.54 Å.

Lattice parameter (a, b, c)

To calculate Lattice constant use following relation [8].

$$\frac{1}{d^2} = \frac{h^2}{a^2} + \frac{k^2}{b^2} + \frac{l^2}{c^2} \quad (13)$$

ISBN: 978-93-95369-55-8 (paperback) 978-93-95369-46-6 (electronic)

for cubic system $a = b = c$

$$a = d(h^2 + k^2 + l^2)^{1/2} \quad (14)$$

Where h, k, l are miller indices of the given plane.

Hopping lengths L_A and L_B

Hopping length is nothing but the distance between magnetic ions. Let L_A is hopping length in tetrahedral sites and L_B is hopping length in octahedral sites. L_A and L_B can calculate from following equations [9].

$$L_A = a(\frac{\sqrt{3}}{4}) \quad (15)$$

$$L_B = a(\frac{\sqrt{2}}{4}) \quad (16)$$

Mean ionic radius r_A and r_B

Let r_A ionic radius of the tetrahedral site and r_B ionic radius of the octahedral site. r_A and r_B can calculate from following equations [9].

$$r_A = a\sqrt{3}(u - 1/4) - R_o \quad (17)$$

$$r_B = a(5/8 - u) - R_o \quad (18)$$

Where $a =$ lattice parameter,

$u =$ oxygen positional parameter for ideal spinel ferrite $=$ 0.375 Å

$R_0 =$ radius of oxygen ion $=$ 1.32 Å

Bond lengths d_{Ax} and d_{Bx}

The bond lengths on the tetrahedral (d_{Ax}) and octahedral (d_{Bx}) sites can calculate from equations [10]

$$d_{Ax} = a\sqrt{3}\left(u - \frac{1}{4}\right) \quad (19)$$

ISBN: 978-93-95369-55-8 (paperback) 978-93-95369-46-6 (electronic)

$$d_{Bx} = a\left(3u^2 - \frac{11}{4}u + \frac{43}{64}\right)^{1/2} \text{ or } a\left(\frac{5}{8} - u\right) \quad (20)$$

Where a = lattice parameter,

R_0 = Ionic radius of the Oxygen ion = 1.38 Å

u = Oxygen parameter = 3/8 for ideal cubic spinel ferrite.

X-ray density

The X-ray density can calculate from following relation [11]

$$\rho_x = \frac{8M}{Na^3} \quad (21)$$

Where, M = molecular weight of the sample, a = lattice parameter,

N = Avogadro number

2. Fourier transform infrared (FTIR**) spectroscopy**

The total internal energy of molecules is addition of vibrational, rotational, and electronic energy levels. In FTIR the electromagnetic radiations (in the IR region) interaction with matter are studied. In the IR region, electromagnetic waves are generally coupled with molecular vibrations. After absorbing IR radiations, the molecules vibrated and attain a higher state. The absorption of IR frequency by sample depends on interaction with molecules. "If IR photon energy is equal to the vibrational energy of the molecule, then it gets absorbed by the material" [12].

Working Principle of FTIR Spectrometer

FTIR spectrometer scans a spectrum of wavelength. In FTIR, monochromator Michelson's interferometer is used. In this case, interference of two beams produces a pattern called an inter ferogram. This is produced because of change in path length between two interfering beams [13]. Figure 2 shows FTIR spectrometer.

Initially, radiations from the IR source fall on the beam splitter. Then beam splitter splits these radiations; 50% of radiations are reflected towards the stationary mirror and 50% of radiations are transmitted towards the movable mirror. After radiations incident on stationary and movable mirror reflected backward toward beam splitter.

If the optical path difference (OPD) between the stationary and movable mirror is $\lambda, 2\lambda, 3\lambda, ...$ then constructive interference is produced. If it is $\lambda/2, 3\lambda/2, 5\lambda/2, ...$ then we get destructive interference at the beam splitter. Therefore, the interferometer is produced a beam, contains waves of varying intensity. These radiations continuously fall on the sample. If falling radiation energy

ISBN: 978-93-95369-55-8 (paperback) 978-93-95369-46-6 (electronic) | © 2025 Advent Publishing.

matches the molecular vibrational energy in the sample, then sample (by vibrating and stretching bonds) absorbed this energy and the remaining energy is transmitted through the sample.

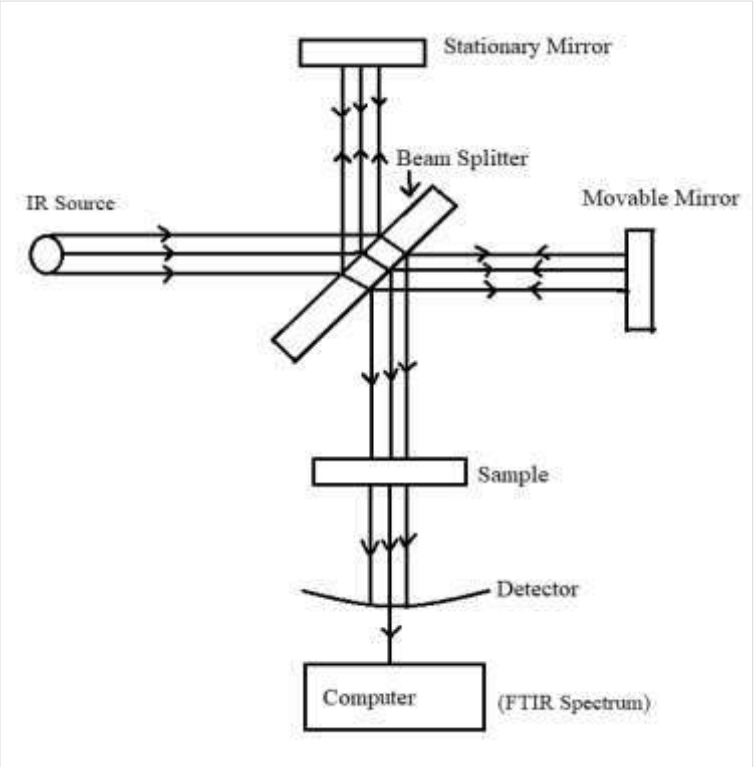

Fig. 2. FTIR Spectrometer

The transmitted radiations are detected by the detector and spectrum is formed called an interferometer (graph of energy Vs time). This signal is fed to a computer that applies Fourier transform equation and converts the time domain into the frequency domain. The FTIR spectrum represents a graph of % transmission or % absorption against wavenumber (cm^{-1}). Infrared (IR) electromagnetic spectrum consist of three regions [14].

a) Far Infrared (400 – 100 cm^{-1}) - It has low energy, used for rotational spectroscopy.

b) Mid-Infrared (4000 – 400 cm^{-1}) - Used to study fundamental vibrations - related to vibration and rotational structure.

c) Near Infrared (14000 – 4000 cm^{-1}) – It has higher energy-related harmonic vibrations.

The different characteristic peaks of the spectrum of the sample identify presence of different groups, molecules, and gives information of crystal structure.

ISBN: 978-93-95369-55-8 (paperback) 978-93-95369-46-6 (electronic)

3. Field-emission scanning electron microscopy (FE-SEM)

"FE-SEM uses an electron beam instead of light to illustrate the object". Therefore, the resolution of SEM is very high in the order of nanometres. Spatial resolution of FE-SEM is 3 to 6 times better than SEM. The magnification of FE-SEM is 10X to 300000X which is much better than SEM. In FE-SEM the electrons are emitted due to field emission therefore this emission is called a cold emission [15].

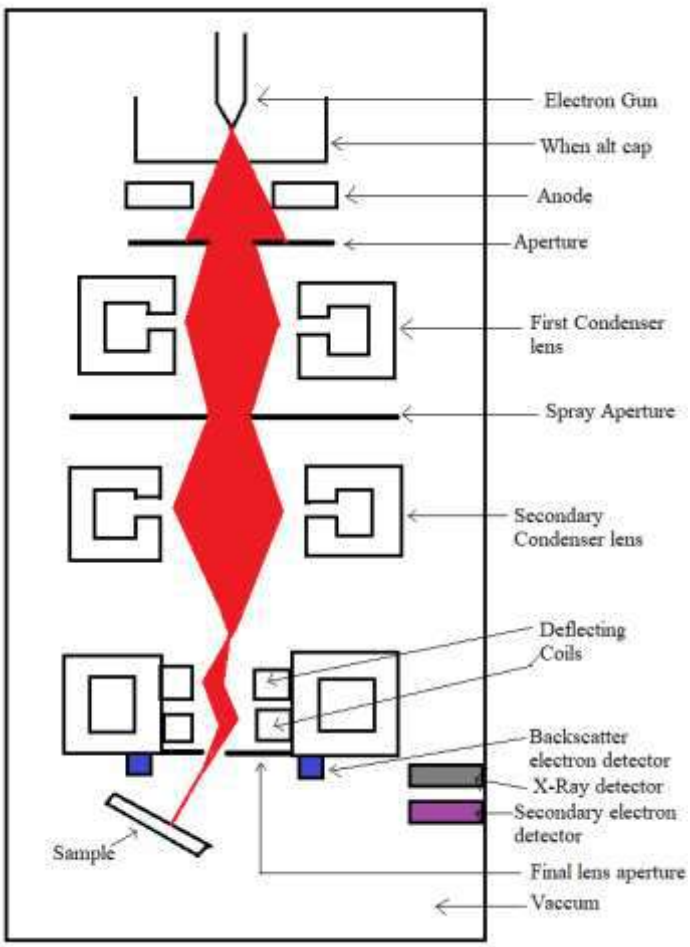

Fig. 3. Schematic diagram of FE-SEM

The cathode emits electrons in FE-SEM because of field emission phenomenon therefore it has high to low energy which gives high spatial resolution and minimum sample damage, electron gun emits electrons are accelerated by applying a high electric field. By using electronic lenses called condenser lenses. Primary emitted electrons are focused and deflected in one direction to obtain sharp narrow electron beam. The electron beam incident on a sample and emits secondary electrons. Secondary electrons are detected and recorded with help of the detector. Secondary electrons detected and produce an

ISBN: 978-93-95369-55-8 (paperback) 978-93-95369-46-6 (electronic)

electrical signal. Using an amplifier, the electrical signal can be amplified. Finally, the electrical signal is transformed into an image. In SEM and FE-SEM secondary electrons gives information of sample morphology and material composition [16]. Figure 3. shows a schematic representation of FE-SEM.

4. Energy dispersive X-ray spectroscopy (EDS)

The energy-dispersive X-ray spectroscopy (EDS) is mainly used to find elementary composition of the material. When electrons beam is bombarded on a sample it is interacts with the shell electron of the atom. The shell electron gets knocked out from the atom. This forms a vacancy in the atom which is filled by highest energy state electron of the neighbouring shell. The higher energy state electron jumps into lowest energy state by emitting radiations called X-rays. The X-rays emitted out are a characteristics of given element [17]. Figure 4 shows X-ray emission by shell electron.

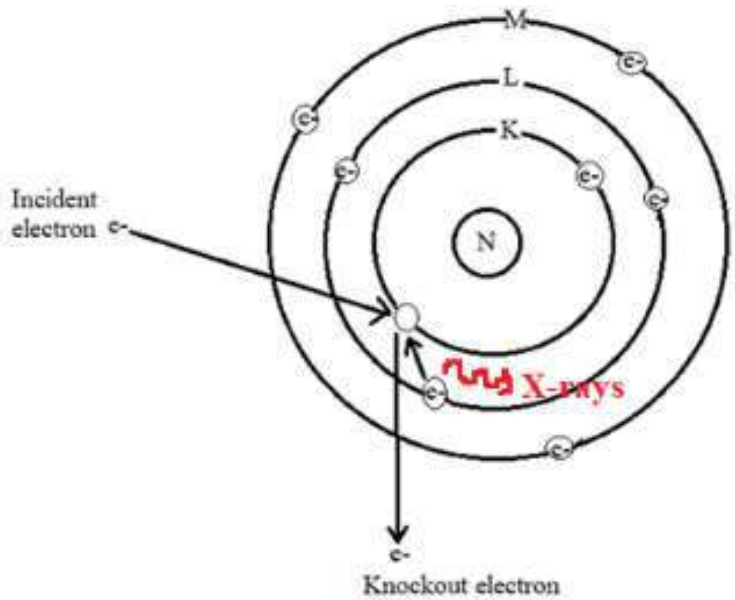

Fig. 4. Schematic diagram of X-ray emission in *EDS*

Continuous and characteristics types of X-rays are emitted depending on incident X-ray energy. The type of X-ray emitted from the sample gives information of elementary composition. It is calculating elements wt. percentage and atomic wt. percentage for selected region of the sample. The emitted X-ray energy rely on electrons transition from one shell to another shell which represents the difference between shells and the atomic structure of the element.

The X-ray detector measure the abundance of X-rays against energy. The emitted X-ray detected by the detector produces a charge pulse which is proportional to the energy of the X-ray. To convert charge pulse into voltage pulse preamplifier is used. Using a multichannel analyser, the voltage signal is

ISBN: 978-93-95369-55-8 (paperback) 978-93-95369-46-6 (electronic)

analysed. The X-ray energy is measured from voltage signal. Finally, the computer displays a spectrum of count Vs energy to determine elementary composition. [18].

5. DC electrical resistivity (ρ) measurement (Two probe method)

The two probe method is very useful to measure the DC electrical resistivity (ρ) of the sample. By using hydraulic press, we can make a pellets of different dimensions by maintaining pressure up to 5 tons/cm^2 for 5-7 minutes. Then, by releasing pressure pellets can be made then polish and paste it by using silver paste to make good ohmic contact for resistivity measurement. After the silver pasted pellets are totally dried then fitted into two electrodes for resistance measurement.

Calculate DC electrical resistivity (ρ) of the sample from following relation [19].

$$\rho_{dc} = \frac{RA}{t} \tag{22}$$

Where A = Area of cross-section of the pellet $= \pi r^2$

t = Thickness of the pellet

R = resistance of the pellet

DC electrical resistivity (ρ) depends on elementary composition, microstructural property, method of preparation, and environmental conditions during preparation [20].

Using Arrhenius equation calculate Activation energy as follows [19]

$$\rho = \rho_0 e^{(\frac{-\Delta E}{kT})} \tag{23}$$

Where ρ_0 = constant, T = Temperature, ΔE = activation energy

Take ln of both sides of equation (23), we get

$$\ln \rho = \ln \rho_0 - \frac{\Delta E}{KT} \tag{24}$$

Plot a graph of $\log \rho$ Vs $1000 / T$ and then calculate activation energy (ΔE) from slope.

6. Dielectric properties

Dielectric materials are insulators. The materials which are non-conducting but store electrical charges are called dielectric materials. Ferrites are dielectric having high resistivity [21]. Polarization is the process in which electrical dipoles are produced inside a dielectric material in presence of an electric field. Ferrites show insulating property which is an active dielectric that allows storage of electrical energy [12]. Figure

ISBN: 978-93-95369-55-8 (paperback) 978-93-95369-46-6 (electronic) | © 2025 Advent Publishing.

5 shows the dipole displacement in dielectric material in the absence and presence of an external electric field.

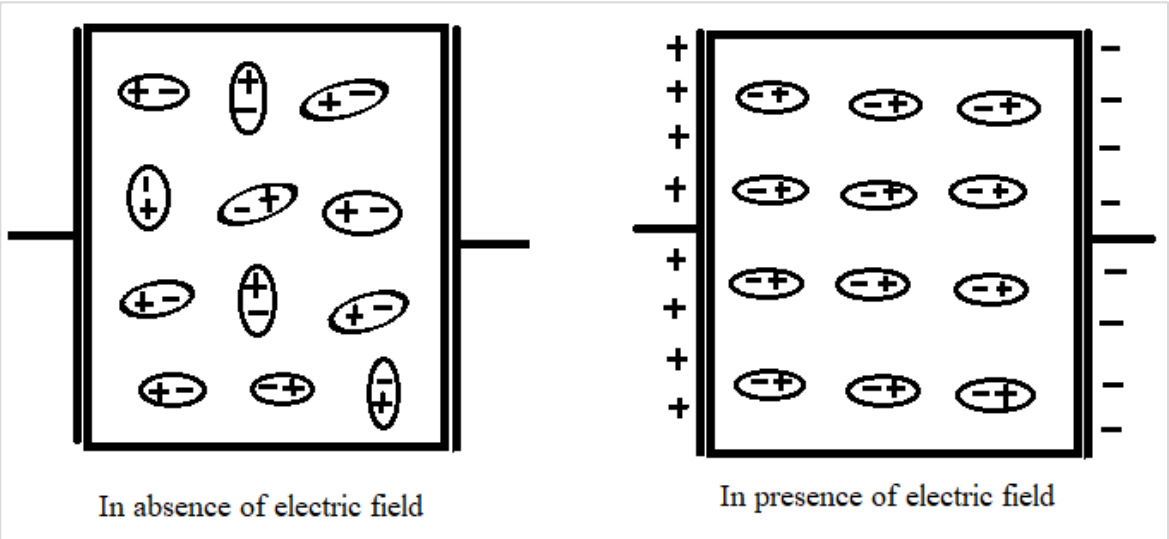

Fig. 5. Dipole displacement in an absence and presence of electric field

There are four different types of polarization possible in the material [22].

- **Electric polarization (Electronic or Atomic polarization)**

In this case, there is the separation of the negative charge electron and positive charge nucleus under applied electric field.

- **Ionic polarization**

This is practicable in solids that have ionic bonding present therefore there is already dipoles existing in solid but cancelled to maintain symmetry of the crystal. If electric field is applied to the material, then ions are displaced from its equilibrium position and produces the resultant dipole moment.

- **Dipolar or Orientation polarization**

In the absence of field, distribution of molecular dipoles is random due to thermal fluctuation. After applying field molecular dipoles are oriented in directions of field.

- **Interface (space charge) polarization**

This is happening generally on the boundaries of the grains and electrode material interfaces. Figure 4.9 shows different types of polarization in the dielectric materials [23].

ISBN: 978-93-95369-55-8 (paperback) 978-93-95369-46-6 (electronic)

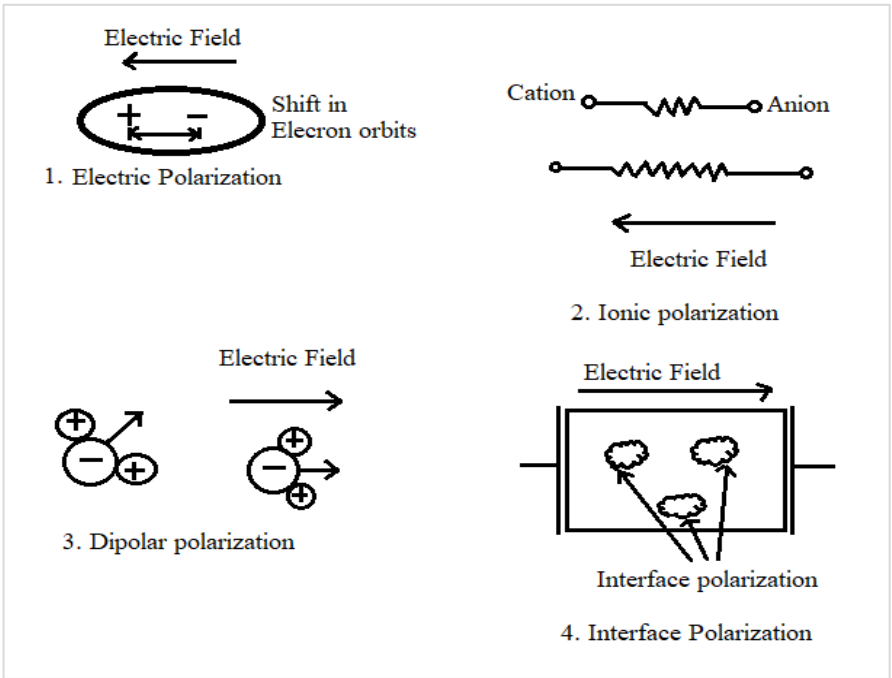

Fig. 6. Different types polarization

Dielectric constant

The characteristics of dielectric materials determine by a parameter called a dielectric constant. Dielectric constant depends on polarization. "The dielectric constant is the ratio of absolute permittivity (ε) of the medium and permittivity of the free space (ε_0)" [24]. Mathematically, written as

$$\varepsilon_r = \varepsilon / \varepsilon_0 \tag{25}$$

For vacuum in plates, the capacitance (C_{Vacuum}) between plates is defined as

$$C_{Vacuum} = \frac{\varepsilon_0 A}{d} \tag{26}$$

$$\varepsilon_0 = 8.85 \times 10^{-12} \, Farad / metre$$

For dielectric medium in plates capacitance (C) between plates is written as

$$C = \frac{\varepsilon A}{d} = \frac{\varepsilon_r \varepsilon_0 A}{d} \tag{27}$$

The relative permittivity (dielectric constant (ε_r)) can be defined as

ISBN: 978-93-95369-55-8 (paperback) 978-93-95369-46-6 (electronic)

$$\varepsilon_r = \frac{C}{C_{Vacuum}} \tag{28}$$

Dielectric constant measures electric charge (polarization) in the dielectric material under applied electric field. Dielectric constant measures the charge holding ability of the materials. It is depending on the temperature, voltage, and frequency of the applied field [24].

ε_r is static dielectric constant in dc field. If ac field is applied to the material, then some amount of energy is utilized for charge storage, and remaining is lost in the form of heat called energy dissipation. Due to thermal oscillations, dipole moments are randomly orientated cannot give an instant response to applied field, hence there are energy losses. Electrical energy absorbed by dielectric material when subject to an applied electric field known as dielectric loss. Therefore, the dielectric constant (ε_r) is represented as [25]

$$\varepsilon_r = \varepsilon_r' - i\varepsilon_r'' \tag{29}$$

Where ε_r' = Real part represents the dielectric constant of material under applied ac field

ε_r'' = Imaginary part representing dielectric losses due to heat dissipation

The ε_r' can be defined as [26]

$$\varepsilon_r' = \frac{C_1 d}{\varepsilon_0 A} \tag{30}$$

Where C_1 = Capacitance of dielectric material under applied ac electric field

A = Area of cross-section; d = Distance between parallel plates

$\varepsilon_0 = 8.85 \times 10^{-12}\, Farad / metre$

Dielectric loss tangent

The dielectric loss tangent can be defined as [26]

$$\tan\delta = \frac{\varepsilon_r''}{\varepsilon_r'} \tag{31}$$

Dielectric loss tangent represents how much energy lost by the material.

ISBN: 978-93-95369-55-8 (paperback) 978-93-95369-46-6 (electronic)

ac Conductivity

The conductivity (σ) of the materials is represented by following equation [27]

$$\sigma = \sigma_{dc}(T) + \sigma_{ac}(\omega, T) \tag{32}$$

The electrical conductivity (σ) of the spinel ferrites depends on the electrons hopping.

Where $\sigma_{dc}(T)$ is dc conductivity of the samples depends on temperature (T). $\sigma_{ac}(\omega, T)$ is the ac conductivity were estimated from following equation [28]

$$\sigma_{ac} = \varepsilon_r' \varepsilon_0 \omega \tan\delta \tag{33}$$

The ac conductivity can be expressed by empirical relation [29]

$$\sigma_{ac} = A\omega^n \tag{34}$$

Where $\omega =$ angular frequency, $n =$ Slope of the $\ln \sigma_{ac} Vs \ln$ *frequency* plot.

Impedance

The impedance of the ferrites can be represented as [30]

$$Z = Z' + Z'' \tag{35}$$

$$Z' = \frac{1/R}{(1/R^2) + \omega^2 C^2} \tag{36}$$

$$Z'' = -\frac{\omega C}{(1/R^2) + \omega^2 C^2} \tag{37}$$

The impedance is contributed due to presence of grains and grain boundaries in the samples [31].

4.2.7 Vibrating Sample Magnetometer (VSM)

The VSM is used for investigation of magnetic properties of materials. The principle and working of VSM based on Faraday's law "i.e. changing magnetic field induce an electric field in the sample" [32]. Figure 7 shows a vibrating sample magnetometer.

Initially, the sample is loaded in sample holder. Then this sample is placed in the uniform magnetic field ($\vec{B}$) produced by electromagnets. In a uniform magnetic field ($\vec{B}$), the sample physically vibrates and produced the oscillatory movement, induces a change in the electric field which is detected by the search coil and measured as a function of time. The electric field measured by sensing coil gives information of change in a magnetic field which is proportional to magnetization [33].

ISBN: 978-93-95369-55-8 (paperback) 978-93-95369-46-6 (electronic) | © 2025 Advent Publishing.

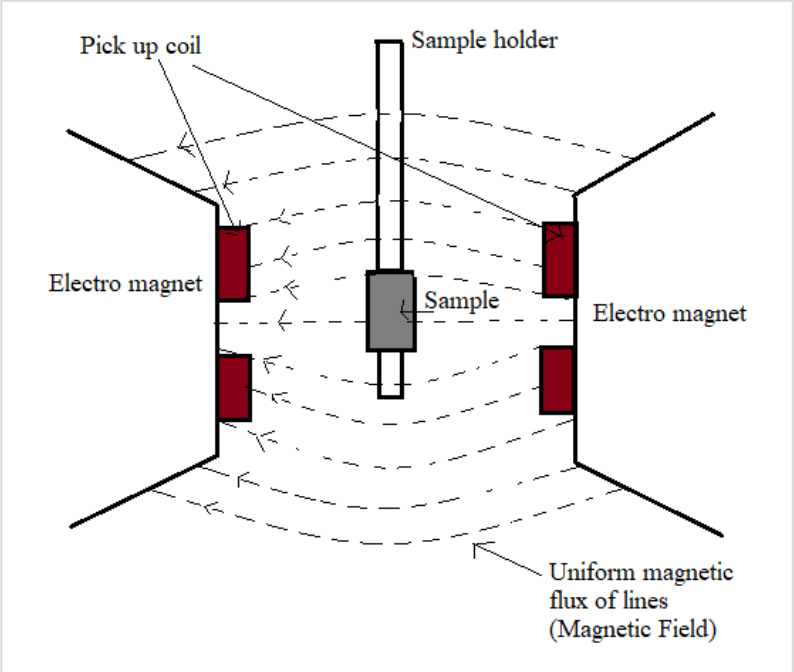

Fig. 7. Vibrating sample magnetometer (*VSM*)

This gives information about different magnetic parameters such as saturation magnetization, coercive field (Coercivity), remanent magnetization (retentivity), isotropic constant, etc.

References

1. https://www.iitk.ac.in/che/pdf/resources/XRD-reading-material
2. D. Kurmude, R. Barkule et al., J. Super. & Novel Magn., 2013, **27(2)**, 547-553. doi:10.1007/s10948-013-2305-2
3. R. Qindeel & N. Alonizan, Current Appl. Phys., 2018, **18(5)**, 519-525. doi:10.1016/j.cap.2018.03.004
4. A. Monshi, M. R. Foroughi et al., World J. Nano Sci. & Engineer., 2012, **2**, 154-160. doi:10.4236/wjnse.2012.23020
5. V. Mote, Y. Purushotham, et al., J. Theo. & Appl. Phys.,2012, **6**, 1-8. doi:10.1186/2251-7235-6-6
6. K. Aly, N. Khalil et al., J. Alloys & Comps., 2016, **676**, 606-612. doi:10.1016/j.jallcom.2016.03.213
7. Sapna, N. Budhiraja, V. Kumar & S. K. Singh, J. Adv. Phys., 2017, **6**, 1–4. doi:10.1166/jap.2017.1363

ISBN: 978-93-95369-55-8 (paperback) 978-93-95369-46-6 (electronic)

8. A. Anwar, S. Zulfiqar et al., J. Mater. Re. & Tech., 2020, **9(3)**, 5313-5325. doi:10.1016/j.jmrt.2020.03.057
9. S. Debnath, K. Deb, B. Saha & R. Das, J. Phys. & Chem. of Solids, 2019, **134**, 105-114. doi:10.1016/j.jpcs.2019.05.047
10. A. Amaliya, S. Anand et al., J. Magn. Magn. Mater., 2018, **467**, 14-28. doi:10.1016/j.jmmm.2018.07.058
11. A. Ati, Z. Othaman & A. Samavati. J. Mole. Struct., 2013, **1052**, 177-182. doi:10.1016/j.molstruc.2013.08.040
12. S. Xavier, Ph.D. Thesis, 2014.
13. Subramanian, Anand & Rodriguez-Saona, Luis. FTIR Spec., Elsevier, 2009, 146-173, doi:10.1016/B978-0-12-374136-3.00007-9.
14. B.M. Cullum & T. Vo-Dinh, Handbook of Spectroscopy, Wiley VCH, 2003. doi:10.1002/3527602305
15. D. Semnani, Electro. Nanofibers, 2017, 151-180. doi:10.1016/b978-0-08-100907-9.00007-6
16. https://www.nanoscience.com/techniques/scanning-electron-microscopy/
17. A. Polini & F. Yang, Nanofiber Composites for Biomedical Apps., 2017, 97-115. doi:10.1016/b978-0-08-100173-8.00005-3
18. C. Colpan, Y. Nalbant & M. Ercelik, Comprehensive Energy Sys., 2018, 1107-1130. doi:10.1016/b978-0-12-809597-3.00446-6
19. I. Gul & A. Maqsood, J. Alloys & Comps., 2008, **465(1-2)**, 227-231. doi:10.1016/j.jallcom.2007.11.006
20. S. Aman, M. Tahir & N. Ahmad, J. of Mater. Sci.: Mater. in Elec., 2021, **32(17)**, 22440-22449. doi:10.1007/s10854-021-06730-8
21. S. Gowreesan & A. Kumar, Chinese J. of Phys., 2018, **56(3)**, 1262-1272. doi:10.1016/j.cjph.2018.02.014
22. J. Dean, Microwave Extract., 2021, 135-149. doi:10.1016/b978-0-12-381373-2.00048-x
23. https://www.slideshare.net/SivanagiReddyEmani/dielectrics-and-microwaves
24. D. Bogdal, Microwave-Assisted Org. Syn., 2005, 1-11. doi:10.1016/s1460-1567(05)80014-5
25. A. Varshneya & J. Mauro, Dielectric properties, 2019, 425-442. doi:10.1016/b978-0-12-816225-5.00015-8
26. Mubasher, M. Mumtaz, et al., Appl. Phys. A, 2020, **126(5)**. doi:10.1007/s00339-020-03529-y

ISBN: 978-93-95369-55-8 (paperback) 978-93-95369-46-6 (electronic)

27. N. Kumari, V. Kumar & S. Singh, RSC Advances, 2015, **5(47)**, 37925-37934. doi:10.1039/c5ra03745j

28. A. Bandyopadhyay, S. Sharma et al., J. Alloys & Comps., 2021, **882**, 160720 (1-11). doi:10.1016/j.jallcom.2021.160720

29. I. Ali, M. Islam et al. J. Elec. Mater., 2013, **43(2)**, 512-521. doi:10.1007/s11664-013-2900-9

30. K. Bharathi, G. Markandeyulu & C. Ramana, J. Electro Chem. Soc., 2011, **158(3)**, G71. doi:10.1149/1.3534800

31. M. Anupama, B. Rudraswamy & N. Dhananjaya, J. Alloys & Comps., 2017, **706**, 554-561. doi:10.1016/j.jallcom.2017.02.241

32. A. Adeyeye & G. Shimon, Magn. of Sur., Inter., & Nanoscale Mater., 2015, 1-41. doi:10.1016/b978-0-444-62634-9.00001-1

33. M. Nasrollahzadeh, M. Atarod et al., Plant-Mediated Green Syn. of Nano-Struct., Elsevier, 2019, **28**, 199-322. doi:10.1016/b978-0-12-813586-0.00006-7

ISBN: 978-93-95369-55-8 (paperback) 978-93-95369-46-6 (electronic)